

Enhanced Superconducting Gaps in the Trilayer High-Temperature $\text{Bi}_2\text{Sr}_2\text{Ca}_2\text{Cu}_3\text{O}_{10+\delta}$ Cuprate Superconductor

S. Ideta,¹ K. Takashima,¹ M. Hashimoto,¹ T. Yoshida,¹ A. Fujimori,¹ H. Anzai,² T. Fujita,² Y. Nakashima,² A. Ino,² M. Arita,³ H. Namatame,³ M. Taniguchi,^{2,3} K. Ono,⁴ M. Kubota,⁴ D. H. Lu,⁵ Z.-X. Shen,⁵ K. M. Kojima,¹ and S. Uchida¹

¹*Department of Physics, University of Tokyo, Bunkyo-ku, Tokyo 113-0033, Japan*

²*Graduate School of Science, Hiroshima University, Higashi-Hiroshima 739-8526, Japan*

³*Hiroshima Synchrotron Center, Hiroshima University, Higashi-Hiroshima 739-0046, Japan*

⁴*Photon Factory, Institute of Materials Structure Science, KEK, Tsukuba, Ibaraki 305-0801, Japan*

⁵*Department of Applied Physics and Stanford Synchrotron Radiation Lightsource, Stanford University, Stanford, California, 94305, USA*

(Received 20 April 2009; published 1 June 2010)

We report the first observation of the multilayer band splitting in the optimally doped trilayer cuprate $\text{Bi}_2\text{Sr}_2\text{Ca}_2\text{Cu}_3\text{O}_{10+\delta}$ (Bi2223) by angle-resolved photoemission spectroscopy. The observed energy bands and Fermi surfaces are originated from the outer and inner CuO_2 planes (OP and IP). The OP band is overdoped with a large d -wave gap around the node of $\Delta_0 \sim 43$ meV while the IP is underdoped with an even large gap of $\Delta_0 \sim 60$ meV. These energy gaps are much larger than those for the same doping level of the double-layer cuprates, which leads to the large T_c in Bi2223. We propose possible origins of the large superconducting gaps for the OP and IP: (1) minimal influence of out-of-plane disorder and a proximity effect and (2) interlayer tunneling of Cooper pairs between the OP and IP.

DOI: 10.1103/PhysRevLett.104.227001

PACS numbers: 74.25.Jb, 71.18.+y, 74.72.-h, 79.60.-i

It has been well known that one of the most efficient ways to increase the critical temperature (T_c) of high- T_c cuprate superconductors (HTSCs) is to increase the number of neighboring CuO_2 planes (n). T_c of the optimally doped region ($T_{c,\text{max}}$) generally increases from single layer ($n = 1$), double layer ($n = 2$), to triple layer ($n = 3$) and then decreases for $n \geq 4$ [1]. In order to explain the n dependence of T_c , several mechanisms have been proposed. According to the theory of tunneling mechanism of Cooper pairs between the CuO_2 planes, $T_{c,\text{max}}$ should increase with increasing n [2]. Furthermore, if one takes into account the charge imbalance between the planes and the existence of competing order, $T_{c,\text{max}}$ takes a maximum at $n = 3$ [3], in agreement with the experiment. Meanwhile, T_c tends to increase with next-nearest-neighbor Cu-Cu hopping parameter t' , which increases with the number of CuO_2 planes [4]. Also, T_c increases with decreasing degree of out-of-plane disorder [5,6]. However, it has been unclear which parameter governs the n dependence of $T_{c,\text{max}}$ because of the lack of detailed knowledge about the electronic structure of the multilayer cuprates.

So far, angle-resolved photoemission spectroscopy (ARPES) studies have been performed for multilayer cuprates such as double-layer Bi2212 [7–9] and four-layer $\text{Ba}_2\text{Ca}_3\text{Cu}_4\text{O}_8\text{F}_2$ (F0234) [10,11], and have revealed the splitting of band dispersions and Fermi surfaces (FSs). In Bi2212, hybridization between the two CuO_2 planes causes band splitting into the bonding and antibonding bands [7]. The ARPES study on F0234 has indicated band splitting due to the different hole concentrations of

the outer and inner CuO_2 planes [10,11], where the maximum superconducting (SC) gap was ~ 60 meV, approximately twice as large as that of the smaller one. However, in the case of triple-layer $\text{Bi}_2\text{Sr}_2\text{Ca}_2\text{Cu}_3\text{O}_{10+\delta}$ (Bi2223) which has the highest $T_{c,\text{max}}$ ($= 110$ K) among Bi-based HTSCs, band splitting and multiple FSs have not been identified in the previous ARPES studies [12–14]. To clarify the role of the multiple CuO_2 planes for the highest T_c , it is important to observe the multiband of triple-layer HTSCs and to compare the electronic structure with those of single- and double-layer cuprates.

In the present Letter, with aid of high-quality single crystals and bulk sensitivity in low-photon-energy ARPES, we have successfully observed the band splitting of Bi2223 and have revealed that the outer (OP) and inner CuO_2 plane (IP) have different doping levels and different gap magnitudes. Furthermore, the SC gaps for the OP and IP are very large compared to those for the same doping levels of Bi2212, which leads to the high $T_{c,\text{max}}$ in Bi2223. We shall discuss the origin of the large SC gaps for the OP and IP and the highest T_c of triple-layer cuprates in relation to the multi- CuO_2 layers.

Single crystals of optimally doped Bi2223 ($T_c = 110$ K) were grown by the traveling solvent floating zone method [15]. ARPES experiments were carried out at BL 9A of the Hiroshima Synchrotron Radiation Center ($h\nu = 6.6\text{--}12.9$ eV, circularly polarized light), BL 5-4 of the Stanford Synchrotron Radiation Laboratory ($h\nu = 18.5$ eV, linear polarized light), BL 28A of the Photon Factory ($h\nu = 45$ eV), and the University of Tokyo (He $I\alpha$ $h\nu = 21.218$ eV). The total energy resolution

(ΔE) was set at 5, 11, 15, and 18 meV, respectively. The samples were cleaved *in situ* under an ultrahigh vacuum of $\sim 1 \times 10^{-11}$ Torr. The measurements were performed at $T = 10$ K.

We show spectral weight mapping integrated within ± 20 meV centered at the Fermi level (E_F) in Figs. 1(a) and 1(b). Two FS sheets corresponding to the OP and IP are successfully resolved, and the intensity of OP is enhanced for $h\nu = 7.65$ eV while that of IP is enhanced for $h\nu = 11.95$ eV. As shown in Fig. 1(e), the intensity ratio of the OP and IP bands deduced from the momentum distribution curve's at E_F in the nodal direction are indeed strongly dependent on photon energy. In particular, in the low-photon energy region, it changes dramatically with small changes in photon energy. Here, we assign the FS sheet closer to the Γ point to the OP, and the other FS sheet to the IP, following the NMR studies of triple-layer HTSCs, where the hole concentration of the OP is found to be larger than that of the IP [16,17].

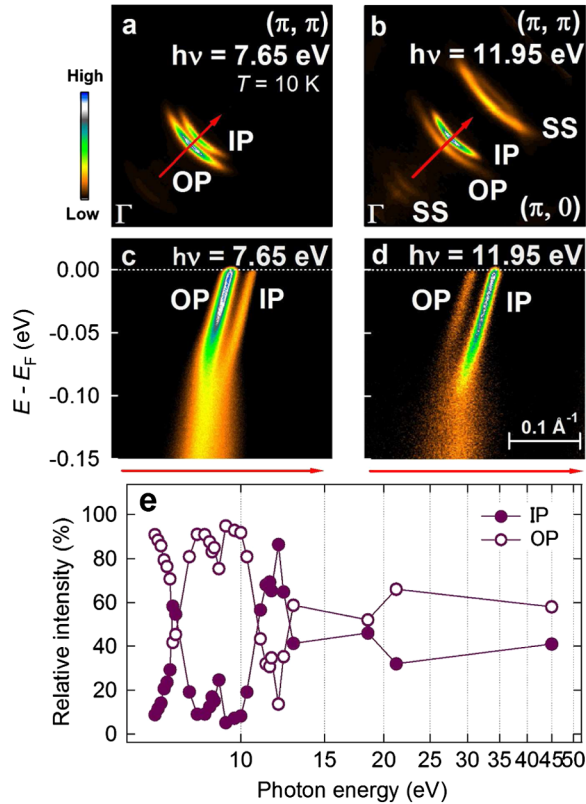


FIG. 1 (color online). (a),(b) Intensity plots of ARPES spectra for Bi2223 at $E = \pm 20$ meV in momentum space. Two Fermi surfaces are observed corresponding to the outer CuO_2 plane (OP) and inner CuO_2 plane (IP). Superstructures due to the Bi-O layer modulation are indicated by SS. (c),(d) Band dispersions in the nodal direction corresponding to red arrows in (a) and (b), respectively. (e) Relative intensities of the OP and IP bands as functions of photon energy. For $h\nu = 7.65$ eV [(a),(c)], the OP band spectra are enhanced while for $h\nu = 11.95$ eV [(b),(d)], the IP band is enhanced.

The dispersions in the nodal direction corresponding to Figs. 1(a) and 1(b) are shown in Figs. 1(c) and 1(d), respectively. Since there are three neighboring CuO_2 planes, one would expect to observe three bands which come from two OP and one IP bands, as indicated by t - t' - t'' - J model calculation [18]. The fact that we observed only two bands implies that the two OP bands, i.e., the bonding and antibonding OP bands, are nearly degenerate. In fact, the FWHM of the momentum distribution curve for the OP band at E_F , ~ 0.011 (\AA^{-1}), is significantly larger than that of the IP band ~ 0.0074 (\AA^{-1}), suggesting that two unresolved OP bands exist. The FWHM of the IP band is nearly the same as that of the bonding or antibonding band in Bi2212, 0.0065 (\AA^{-1}) [9], indicating its single-component nature. Even in the off-nodal region, splitting of the OP band has not been observed, possibly due to the small interlayer hopping [19]. The Fermi momentum (k_F) positions for the OP and IP have been determined by the minimum-gap locus in the SC state [20]. The k_F 's were fitted by the tight-binding model, yielding the values of tight-binding parameters $-t'/t \sim 0.26$ (OP) and ~ 0.29 (IP), if the third-nearest-neighbor hopping parameter is assumed to be $-t''/t = 0.5$ [4]. The hole concentration for the OP and IP bands deduced from the FS areas are $\sim 23\%$ and $\sim 7\%$, respectively. The average hole concentration is $\sim 18\%$ taking into account the number of CuO_2 layers.

We show dispersions in the SC state for the OP and IP bands, respectively, from the nodal to off-nodal cuts in Figs. 2(a) and 2(b). The gap energies for both bands are very different, as in the case of F0234 ($n = 4$). The gap magnitudes for the OP and IP bands have been estimated from the peak position of the symmetrized energy distribution curve at each k_F fitted to the phenomenological model [21,22]. The momentum dependence of the gap magnitude for OP is almost simple d wave, $\Delta_0 |\cos(k_x a) - \cos(k_y a)|/2$ with $\Delta_0 \sim 43$ meV, as shown by a straight line in Fig. 2(c). On the other hand, the gap for the IP band deviates from the simple d wave around the antinode $\sim (\pi, 0)$. The gap size is characterized by two parameters $\Delta_0 \sim 60$ meV around the node and $\Delta^* \sim 80$ meV in the antinodal region, where Δ_0 and Δ^* are defined by the linear extrapolation of the gap magnitude to the antinode [$|\cos(k_x a) - \cos(k_y a)|/2 = 1$], as shown in Fig. 2(c). The deviation of the gap anisotropy from the simple d wave is known to be prominent in underdoped cuprates, which is called “two-gap behavior” [22–25]. These observed gap anisotropies are in accord with the doping levels of the OP and IP estimated from the FS areas. Judging from the present result on the gap of OP, $\Delta_0 \sim 43$ meV, one can conclude that the previous ARPES result $\Delta_0 \sim 40$ meV for Bi2223 reflected the OP band due to the employed photon energies of ~ 22 eV [12–14,26].

Δ_0 and Δ^* for $\text{La}_{2-x}\text{Sr}_x\text{CuO}_4$ (LSCO, $n = 1$), Bi2212 ($n = 2$), and Bi2223 ($n = 3$) are plotted as functions of hole doping in Fig. 3. Hole concentrations for the OP and

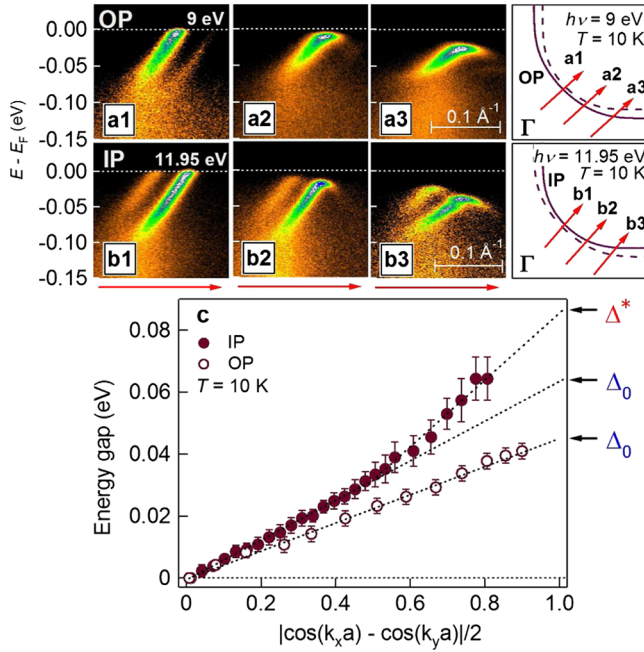


FIG. 2 (color online). Energy-momentum intensity plots for cuts from the nodal to the off-nodal regions for the OP band [(a1)–(a3)] and for the IP band [(b1)–(b3)]. The corresponding cuts are shown in the right panels. The photon energies, $h\nu = 9$ eV and 11.95 eV, enhance the OP and IP bands, respectively. (c) Momentum dependences of the energy gaps. The definition of the SC gap Δ_0 and the antinodal gap Δ^* is shown.

IP were deduced from the FS area. It is clear that the Δ_0 for the OP and IP are very large compared to those for the same doping level of Bi2212. In spite of its heavily overdoping, the Δ_0 of the OP band is almost the same as that of optimally doped Bi2212. Furthermore, the Δ_0 of the IP is much larger than that of underdoped Bi2212. The interpolated values of the Δ_0 of the OP and IP to the average doping $x \sim 0.18$ deduced from the present result, ~ 50 meV, is larger than $\Delta_0 \sim 40$ meV of Bi2212 in the optimally doped region by $\sim 20\%$, whose ratio almost coincides with the T_c ratio between Bi2223 and Bi2212. One can see that the Δ_0 for the same doping level increases with increasing n from $n = 1$ to $n = 3$ while Δ^* weakly increases. Thus, we conclude that the larger size of Δ_0 leads to the higher T_c of ~ 110 K in Bi2223 than those in LSCO and Bi2212.

Now, let us discuss possible origins of the enhancement of Δ_0 in Bi2223 compared with those in the single- and double-layer cuprates shown in Fig. 3. We may consider three possible origins: (1) the values of the next-nearest-neighbor hopping parameter $-t'/t$ which has correlation with $T_{c,\max}$ [4], ~ 0.26 for OP, and ~ 0.29 for IP, is larger than those of the single-layer ($-t'/t \sim 0.15$ – 0.2) [27,28] and double-layer ($-t'/t \sim 0.24$) [29] cuprates; (2) out-of-plane disorder effect is small in IP because IP is protected from the out-of-plane disorder by the OP, and therefore, IP is ideally flat [5]; and (3) interlayer tunneling of Cooper

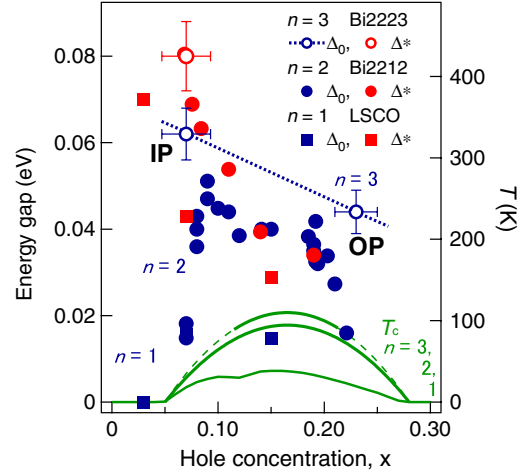


FIG. 3 (color online). Comparison of Δ_0 and Δ^* between the single-, double-, and triple-layer cuprates as functions of hole concentration. Their T_c are plotted by solid curves. The Δ_0 and Δ^* values for $n = 1$ and 2 have been taken from ARPES results for LSCO [24] and Bi2212 [7,22,23,39,40]. The error bars in the hole concentrations reflect uncertainties in the k_F positions.

pairs between OP and IP may enhance the SC order parameter [3].

In Fig. 4, we test the correlation between $T_{c,\max}$, SC gap Δ_0 , $-t'/t$ at optimal doping ($x \sim 0.16$) [30], and Δ^* in the underdoped region ($x \sim 0.07$) [31] for the single-layer (Bi2201, LSCO), double-layer (Bi2212), and triple-layer (Bi2223) HTSCs. One can see a remarkable correlation between Δ_0 and $T_{c,\max}$, that is, $T_{c,\max}$ is nearly proportional to Δ_0 . On the other hand, $T_{c,\max}$ and Δ^* shows only weak correlation compared with $T_{c,\max}$ versus Δ_0 . $-t'/t$ shows some correlation with $T_{c,\max}$, but not so strong as $T_{c,\max}$ versus Δ_0 . In this context, it is interesting to point out that Δ^* is weakly dependent on $-t'/t$, and therefore the large Δ^* of IP can be explained by its large $-t'/t$ value as shown in the inset of Fig. 4 [32]. Such a dependence of Δ^* on $-t'/t$ has been predicted by a t - t' - J model calculation [34]. The out-of-plane disorder may enhance Δ^* [25,35], however, the large Δ^* of IP cannot be explained by this effect since IP is protected from the out-of-plane disorder.

In Bi2223, Δ_0 for IP is very large possibly due to the protection from the out-of-plane disorder by the presence of OPs. Δ_0 for OP is also larger than that in overdoped Bi2212 despite the influence of the out-of-plane disorder to the same extent as in the case of Bi2212. This unusually large Δ_0 of OP can be explained by a proximity effect from IP with the very large Δ_0 [36]. Such a proximity effect would in turn reduce the Δ_0 of IP. The fact that the Δ_0 of IP is nevertheless very large means that the “original” Δ_0 of IP was even larger, or that the proximity effect did not reduce the Δ_0 of IP. Finally, we consider the interlayer tunneling of Cooper pairs which enhances the SC order parameter and hence T_c [3]. In the single-layer cuprates, the tunneling of interlayer Cooper pairs observed by opti-

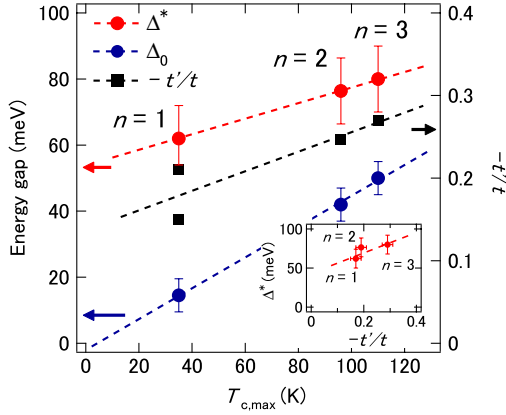


FIG. 4 (color online). Correlation between Δ_0 , $-t'/t$ at optimal doping ($x \sim 0.16$), Δ^* in the underdoped region ($x \sim 0.06$), and $T_{c,\max}$ from the single- ($n = 1$) to triple-layer ($n = 3$) cuprates. Δ_0 shows the strongest correlation with $T_{c,\max}$ ($T_{c,\max} \propto \Delta_0$) while $-t'/t$ and Δ^* show only weak correlation with $T_{c,\max}$. Values of $-t'/t$ for $n = 1$ and 2 have been taken from ARPES results for LSCO [27], Bi2201 [28], and Bi2212 [29]. Inset shows correlation between Δ^* and $-t'/t$ at $x \sim 0.07$. The $-t'/t$ values for $n = 1, 2$ in the inset are taken from Ref. [27] for LSCO and Refs. [29,33] for Bi2212.

cal conductivity is known to have negligible effect on T_c [37]. On the other hand, the effect of intramultilayer tunneling of Cooper pairs on T_c (and Δ_0) remains to be clarified in future studies.

Nonetheless, due to the strong phase fluctuations in the underdoped IP, T_c may be reduced compared to the large pairing amplitude of IP. Kivelson examined a system with alternating two CuO_2 planes as a model of multilayer cuprates [38]; one plane has a large SC gap but a very low superfluid density, and the other one has a very small SC gap but a high superfluid density. The result shows that phase stiffness of the low-superfluid-density plane is increased through coupling with the high-superfluid-density plane, which causes the enhancement of Δ_0 and T_c . Therefore, we consider that this mechanism explains the high T_c of the triple-layer Bi2223 in spite of the strong phase fluctuations in the IP.

In conclusion, we have performed ARPES of the optimally doped Bi2223 and revealed the electronic structure of the outer and inner CuO_2 planes and Fermi surfaces separately. We find that the OP and IP have different hole concentrations with different magnitudes of the gaps. The large nodal Δ_0 for the OP and IP bands explains the large T_c in Bi2223. The possible origins of the large Δ_0 are (1) due to the negligible influence of out-of-plane disorder and a proximity effect and (2) the interlayer tunneling of Cooper pairs. Which mechanism is dominant needs to be clarified in future studies.

We thank C. Panagopoulos, T.P. Devereaux, S. Okamoto, and M. Mori for an informative discussion. ARPES experiments were carried out at HiSOR,

Hiroshima Synchrotron Radiation Center, Hiroshima University (Proposal No. 07-A-10), at KEK-PF (Proposal No. 2006S2-001), and at SSRL (Proposal No. 3230). This work was supported by a Grant-in-Aid for Scientific Research in Priority Area ‘‘Invention of Anomalous Quantum Materials,’’ A3 Foresight Program from Japan Society for the Promotion of Science, and a Global COE Program ‘‘the Physical Sciences Frontier,’’ MEXT, Japan.

- [1] A. Iyo *et al.*, *J. Phys. Soc. Jpn.* **76**, 094711 (2007).
- [2] J.M. Wheatley *et al.*, *Nature (London)* **333**, 121 (1988).
- [3] S. Chakravarty *et al.*, *Nature (London)* **428**, 53 (2004).
- [4] E. Pavarini *et al.*, *Phys. Rev. Lett.* **87**, 047003 (2001).
- [5] H. Eisaki *et al.*, *Phys. Rev. B* **69**, 064512 (2004).
- [6] K. Fujita *et al.*, *Phys. Rev. Lett.* **96**, 097006 (2006).
- [7] D.L. Feng *et al.*, *Phys. Rev. Lett.* **86**, 5550 (2001).
- [8] A.A. Kordyuk *et al.*, *Phys. Rev. B* **70**, 214525 (2004).
- [9] T. Yamasaki *et al.*, *Phys. Rev. B* **75**, 140513(R) (2007).
- [10] Y. Chen *et al.*, *Phys. Rev. Lett.* **97**, 236401 (2006).
- [11] Y. Chen *et al.*, *Phys. Rev. Lett.* **103**, 036403 (2009).
- [12] T. Sato *et al.*, *Phys. Rev. Lett.* **89**, 067005 (2002).
- [13] D.L. Feng *et al.*, *Phys. Rev. Lett.* **88**, 107001 (2002).
- [14] H. Matsui *et al.*, *Phys. Rev. B* **67**, 060501(R) (2003).
- [15] T. Fujii *et al.*, *J. Cryst. Growth* **223**, 175 (2001).
- [16] H. Kotegawa *et al.*, *J. Phys. Chem. Solids* **62**, 171 (2001).
- [17] A. Trokiner *et al.*, *Phys. Rev. B* **44**, 2426 (1991).
- [18] M. Mori, T. Tohyama, S. Maekawa, *Phys. Rev. B* **66**, 064502 (2002).
- [19] S. Ideta *et al.*, *Physica C (Amsterdam)* (to be published).
- [20] M.R. Norman *et al.*, *Nature (London)* **392**, 157 (1998).
- [21] M.R. Norman *et al.*, *Phys. Rev. B* **57**, R11093 (1998).
- [22] W.S. Lee *et al.*, *Nature (London)* **450**, 81 (2007).
- [23] K. Tanaka *et al.*, *Science* **314**, 1910 (2006).
- [24] T. Yoshida *et al.*, *Phys. Rev. Lett.* **103**, 037004 (2009).
- [25] M. Hashimoto *et al.*, *Phys. Rev. B* **79**, 144517 (2009).
- [26] T. Sato *et al.*, *Phys. Rev. Lett.* **91**, 157003 (2003).
- [27] T. Yoshida *et al.*, *J. Phys. Condens. Matter* **19**, 125209 (2007).
- [28] M. Hashimoto *et al.*, *Phys. Rev. B* **77**, 094516 (2008).
- [29] W.S. Lee *et al.*, [arXiv:0606347v](https://arxiv.org/abs/0606347v).
- [30] For $n = 3$, values interpolated between IP and OP have been used.
- [31] We have plotted the Δ^* values for LSCO and Bi2212 at $x \sim 0.06$ in Fig. 3.
- [32] As for the $-t'/t$ of Bi2212 in the inset of Fig. 4, we have plotted the extrapolated value at $x \sim 0.06$ from $-t'/t \sim 0.24$ at $x \sim 0.16$ (Ref. [29]) and ~ 0.20 at $x \sim 0.1$ (Ref. [33]).
- [33] A.A. Kordyuk *et al.*, *Phys. Rev. B* **67**, 064504 (2003).
- [34] P. Prelovšek and A. Ramsak, *Phys. Rev. B* **65**, 174529 (2002).
- [35] Y. Okada *et al.*, *J. Phys. Soc. Jpn.* **77**, 074714 (2008).
- [36] S. Okamoto and T.A. Maier, *Phys. Rev. Lett.* **101**, 156401 (2008).
- [37] J. Schützmann *et al.*, *Phys. Rev. B* **55**, 11118 (1997).
- [38] S.A. Kivelson, *Physica (Amsterdam)* **318B**, 61 (2002).
- [39] J. Mesot *et al.*, *Phys. Rev. Lett.* **83**, 840 (1999).
- [40] H. Ding *et al.*, *Phys. Rev. Lett.* **87**, 227001 (2001).